

Insertion Reactions of Silylenoid Ph₂SiLi(OBu-*t*) into X–H Bonds (X = F, OH, and NH₂)

Ju Xie, Dacheng Feng,* Maoxia He, and Shengyu Feng

Institute of Theoretical Chemistry, Shandong University, Jinan 250100, People's Republic of China

Received: June 19, 2005; In Final Form: September 13, 2005

The insertion reactions of silylenoid [(*tert*-butoxy)diphenylsilyl]lithium Ph₂SiLi(OBu-*t*) into HF, H₂O, and NH₃ molecules have been studied by using density functional theory at the B3LYP/6-31G(d) level. To better understand the reactivity of silylenoid Ph₂SiLi(OBu-*t*), its two most stable isomers, the *p*-complex (**1**) and the three-membered ring (**2**), were selected for reactants. Natural bond orbital (NBO) analysis has been performed to study the effects of charge transfer and to understand the nature of different interactions between atoms or groups. The results indicate that (i) the insertion of Ph₂SiLi(OBu-*t*) into X–H bond proceeds in a concerted manner via a three-membered-ring transition state to form substituted silane Ph₂SiHX with dissociation of LiOBu-*t*; (ii) the activation barrier increases in the order of HF < H₂O < NH₃, and the barrier heights of the **1** insertions are higher than those of the **2** insertions, respectively; (iii) both **1** and **2** display amphiphilic character in their insertion reactions.

1. Introduction

Silylenoid (R₁R₂SiMX), a compound in which an electro-positive metal (M) and a leaving group (X) are bound to the same silicon atom, have been confirmed to be existent and to be one of the important active intermediates in organosilicon chemistry. Therefore, silylenoid has received more and more attention, both experimental and theoretical. In 1980, Clark et al.¹ studied the isomers of lithofluorosilylenoid H₂SiLiF by using *ab initio* calculations for the first time. During recent years, we have systematically studied some silylenoids by using quantum chemistry methods, investigating their structures and reactivity.² In 1995, Tamao et al.³ reported the first experimental study of silylenoid chemistry, detecting the existence of silylenoid [(*tert*-butoxy)diphenylsilyl]lithium, Ph₂SiLi(OBu-*t*). They found that Ph₂SiLi(OBu-*t*) behaves as a silylenoid in some reactions. Most recently, Lee et al.⁴ reported the syntheses of stable halosilylenoids (Tsi)X₂SiLi (Tsi = C(SiMe₃)₃, X = Br, Cl) at room temperature. Since then, further experimental studies on silylenoids have been carried out.⁵ The results of both experimental and theoretical research show that silylenoids exhibit amphiphilic character, nucleophilicity and electrophilicity, and can take part in many reactions. Such reactions as insertion, addition, and polymerization were recognized as important and effective methods for preparation of the new silicon-bonded and heterocyclic silicon compounds.

Nevertheless, theoretical studies on reactions of silylenoids are still quite limited.^{2a–c,6} Feng et al.^{2a,b} reported two insertion reactions of silylenoids H₂SiLiF and H₂SiLiCl into H₂. To the best of our knowledge, there is no systematic study of silylenoid insertion into the polar bonds of small molecules. In this paper, the first experimentally detected silylenoid Ph₂SiLi(OBu-*t*) is chosen to investigate the mechanism of its insertion into HF, H₂O, and NH₃ by using theoretical methods. Most recently, we theoretically studied the structures and isomerization of silylenoid Ph₂SiLi(OBu-*t*).^{2d} It is indicated that the *p*-complex (**1**) and the three-membered-ring (**2**) structures are the two most stable isomers, in which Ph₂SiLi(OBu-*t*) exists and takes part

in chemical reactions. So, structures **1** and **2** were adopted for this study. We hope to obtain a detailed understanding of the mechanism and the reactivity of silylenoid insertion into the polar bonds.

2. Computational Methods

Optimized geometries and energies for the stationary points were obtained by using density functional theory at the B3LYP/6-31G(d) level.⁸ The corresponding harmonic vibrational frequency calculations at the same level were carried out in order to verify whether the stationary points are local minima or saddle points. To verify that transition states actually connect to the expected reactants, intermediates, or products, intrinsic reaction coordinate (IRC)⁹ calculations were performed at the B3LYP/6-31G(d) level with a step size of 0.1 (amu)^{1/2} bohr. Natural bond orbital (NBO)¹⁰ analyses at the B3LYP/6-31G(d) level were then used to demonstrate the charge transfer during the insertion reactions. The *Gaussian 03* series of programs¹¹ were employed in all calculations.

3. Results and Discussion

Table 1 list the total and relative energies calculated at the B3LYP/6-31G(d) level together with the zero-point energies (ZPEs). The term “relative energy” in the following means the energy of a species relative to the reactant in the same reaction. Unless stated otherwise, the reported energies in this paper are computed on the B3LYP/6-31G(d) level, which do not include ZPEs. Table 2 lists the NBO analysis results, the natural charges for atoms or groups, and the occupancy numbers of the lone-pair (LP_{Si}) and anti-lone-pair (LP*_{Si}) orbitals on the Si atom. The frontier molecular orbital analyses (HOMO and LUMO) of silylene Ph₂Si, the *p*-complex (**1**) and the three-membered-ring (**2**) isomers of silylenoid Ph₂SiLi(OBu-*t*), are given in Figure 1. The structures of the stationary points along the reaction paths (see Scheme 1), the reactants, precursor complexes, transition states, insertion intermediates, and products are displayed in Figures 3 and 4 (for **1** + XH reactions) and Figure 6 (for **2** + XH reactions). The potential energy curves are shown in Figure 5 (for **1** + XH reactions) and Figure 7 (for **2** + XH reactions).

* Corresponding author. Tel. +86-0531-8836-5748; Fax +86-0531-8856-4464. E-mail address: fdc@sdu.edu.cn.

TABLE 1: Total Energies E (au) and Relative Energies (in parentheses, kJ/mol) of Various Structures at the B3LYP/6-31G(d) Level

	E	ZPE	$E + ZPE$
1	-993.45696	0.31066	-993.14630
1+HF	-1093.87713 (0.0)	0.31972	-1093.55741 (0.0)
1FC1	-1093.89842 (-55.9)	0.32230	-1093.57607 (-49.0)
1FT	-1093.87761 (-1.3)	0.31891	-1093.55870 (3.4)
1FC2	-1093.96824 (-239.2)	0.32341	-1093.64484 (-229.5)
Ph₂SiHF+3^a	-1093.94601 (-180.8)	0.32083	-1093.62518 (-177.9)
1+H₂O	-1069.86591 (0.0)	0.33183	-1069.53408 (0.0)
1OC1	-1069.87877 (-33.8)	0.33444	-1069.54433 (-26.9)
1OT	-1069.83261 (87.4)	0.33032	-1069.50229 (83.5)
1OC2	-1069.91741 (-135.2)	0.33419	-1069.58312 (-129.0)
Ph₂SiHOH+3	-1069.90579 (-104.7)	0.33180	-1069.57398 (-104.8)
1+NH₃	-1050.00491 (0.0)	0.34520	-1049.65971 (0.0)
1NC1	-1050.01251 (-20.0)	0.34714	-1049.66537 (-14.9)
1NT	-1049.94102 (167.7)	0.34109	-1049.59993 (157.0)
1NC2	-1050.02786 (-60.3)	0.34620	-1049.68166 (-57.6)
Ph₂SiHNH₂+3	-1050.02280 (-47.0)	0.34432	-1049.67848 (-49.3)
2	-993.44520	0.31097	-993.13422
2+HF	-1093.86537 (0.0)	0.32003	-1093.54534 (0.0)
2FC1	-1093.87975 (-37.8)	0.32260	-1093.55715 (-31.0)
2FT	-1093.86884 (-9.1)	0.31887	-1093.54997 (-12.2)
2FC2	-1093.95449 (-234.0)	0.32304	-1093.63146 (-226.1)
Ph₂SiHF+3	-1093.94601 (-211.7)	0.32083	-1093.62518 (-209.6)
2+H₂O	-1069.85415 (0.0)	0.33214	-1069.52201 (0.0)
2OC1	-1069.86533 (-29.4)	0.33492	-1069.53041 (-22.1)
2OT	-1069.82715 (70.9)	0.33036	-1069.49680 (66.2)
Ph₂SiHOH+3	-1069.90579 (-135.6)	0.33180	-1069.57398 (-136.5)
2+NH₃	-1049.99314 (0.0)	0.34551	-1049.64764 (0.0)
2NC1	-1049.99536 (-5.8)	0.34772	-1049.64763 (0.0)
2NT	-1049.94078 (137.5)	0.34196	-1049.59882 (128.2)
Ph₂SiHNH₂+3	-1050.02280 (-77.9)	0.34432	-1049.67848 (-81.0)

^a 3 = LiOBu-*t*.**TABLE 2: Natural Charges for Atoms or Groups and Occupancy Numbers for the Lone-Pair Orbital (LP_{Si}) and Anti-Lone-Pair Orbital (LP*_{Si}) on Si Atom in Various Structures at the B3LYP/6-31G(d) Level**

	Ph ₂	Si	O	Bu- <i>t</i>	H	X	LP _{Si}	LP* _{Si}
1	-1.220	1.009	-1.019	0.345			1.844	0.237
LiOBu-<i>t</i>			-1.113	0.238				
X = F								
HF					0.536	-0.536		
1FC1	-1.164	0.987	-1.009	0.355	0.512	-0.574	1.791	0.259
1FT	-1.078	1.345	-1.017	0.360	0.121	-0.639		0.301
1FC2	-1.055	1.781	-1.045	0.313	-0.238	-0.679		
Ph₂SiHF	-0.932	1.795			-0.239	-0.624		
X = OH								
H₂O					0.466	-0.466		
1OC1	-1.195	0.974	-1.014	0.350	0.480	-0.483	1.834	0.252
1OT	-1.082	1.366	-1.023	0.348	0.082	-0.598		0.321
1OC2	-1.046	1.748	-1.039	0.303	-0.248	-0.641		
Ph₂SiHOH	-0.925	1.744			-0.239	-0.580		
X = NH₂								
1NH₃					0.370	-0.370		
1NC1	-1.211	0.986	-1.013	0.344	0.388	-0.381	1.842	0.242
1NT	-1.082	1.381	-1.026	0.341	0.029	-0.548		0.346
1NC2	-1.162	1.756	-1.017	0.332	-0.293	-0.537		
Ph₂SiHNH₂	-0.915	1.663			-0.237	-0.511		
2	-1.026	0.863	-1.023	0.341			1.806	0.261
2FC1	-1.046	0.864	-1.023	0.342	0.559	-0.550	1.816	0.259
2FT	-0.979	1.303	-1.038	0.350	0.125	-0.637		0.299
2FC2	-1.009	1.874	-1.048	0.308	-0.381	-0.672		
2OC1	-1.025	0.843	-1.021	0.346	0.479	-0.477	1.798	0.272
2OT	-0.992	1.333	-1.036	0.337	0.091	-0.582		0.322
2NC1	-1.057	0.847	-1.025	0.324	0.391	-0.312	1.807	0.287
2NT	-1.013	1.318	-1.033	0.321	0.085	-0.519		0.348

We will first describe and discuss the results of **1** and **2** insertion reactions in subsections 3.1 and 3.2, and then compare the insertion reactivity of **1** with that of **2** in subsection 3.3.

3.1. Insertions of **1 into X-H bonds (X = F, OH, and NH₂).** The calculation^{2d} has shown that the *p*-complex structure

1 is the most stable isomer of four isomers of silylenoid Ph₂-SiLi(OBu-*t*). **1** can be regarded as a complex of the singlet Ph₂-Si with LiOBu-*t* (see Figure 1). The lone pair 2p electrons of the O atom in LiOBu-*t* donate toward the unoccupied p orbital (LUMO) of Si atom in Ph₂Si. In **1**, there also exists an interaction between the positive Li atom and two benzene rings. These effects make **1** stable. As shown in Figure 1, the main component of the HOMO concentrate on the Si atom (the σ orbital LP_{Si} with occupancy number of 1.844) and that of the LUMO concentrate on the Li atom with a part of it on the Si atom (the p orbital LP*_{Si} with occupancy number of 0.237). Namely, **1** can exhibit ambiphilic character, nucleophilicity in its σ orbital direction, and electrophilicity in its p orbital direction. In addition, the σ orbital on the Si atom is exposed, and there exists enough space under the Si atom where the insertions of **1** into X-H bonds takes place.

3.1.1. Precursor Complexes. When the σ orbital (HOMO) of XH as a nucleophile attacks the p orbital on the Si atom from the back of the O atom, the precursor complex forms. Meanwhile, there also exists an interaction between the positive H atom (LUMO) of the X-H bond and the σ orbital on Si (see Figure 2 (1)). As shown in Figures 3 and 4, these precursor complexes, **1FC1**, **1OC1**, and **1NC1**, appear to have similar structures including a loose three-centered bond Si - - H-X. The Si - - H distance increases in the order of **1FC1** (2.234 Å) < **1OC1** (2.583 Å) < **1NC1** (2.879 Å), and the Si - - X interaction is very weak. Relative to the corresponding reactants **1** and XH, there is little variation in the structural parameters of Ph₂SiLi-(OBu-*t*) and XH moieties in precursor complexes. However, it can be found from Table 2 that the donation of σ electrons of XH into the p orbital on the Si atom does occur. In comparison with that of **1**, the positive charge of the Si atom decreases by 0.022 (**1FC1**), 0.035 (**1OC1**), and 0.023 (**1NC1**), which corresponds to the occupancy number of LP*_{Si} increasing by 0.022 (**1FC1**), 0.015 (**1OC1**), and 0.005 (**1NC1**), and that of LP_{Si} decreasing slightly. The stability energy (relative to the corresponding reactants) decreases in the order of **1FC1** (55.9 kJ/mol) > **1OC1** (33.8 kJ/mol) > **1NC1** (20.0 kJ/mol). The formation of the precursor complex is the first step in the course of the **1** insertion reactions. The complexation energy trend demonstrates that **1** can readily undergo interaction with HF.

3.1.2. Transition States. As XH further approaches the p orbital on the Si atom, the positive H atom moves toward the σ orbital on the Si atom so that the σ electrons are partially donated into the antibonding σ^* orbital (H atom) of XH to reach the transition state (see Figure 2 (1)). The optimized transition states, **1FT**, **1OT**, and **1NT** are given in Figures 3 and 4 (the oxygen in water marked as O*), whose single imaginary vibrational frequency is 1084i cm⁻¹(**1FT**), 1289i cm⁻¹(**1OT**), and 1301i cm⁻¹(**1NT**). It should be mentioned that the primary similarity in the three transition states is the three-centered pattern involving Si, H, and the center atom of the X group. The Si-H and Si-X distances in **1FT**, **1OT**, and **1NT** are (29.1%, 21.7%), (39.0%, 30.7%), and (45.9%, 36.2%) shorter than those in the corresponding precursor complexes, respectively. Additionally, the distances of the X-H bond to be broken are 36.9% (**1FT**), 46.0% (**1OT**), and 54.7% (**1NT**) longer than that of the corresponding precursor complexes. All these features indicate that the HF insertion reaction arrives at the transition state relatively early, whereas the NH₃ insertion reaction reaches the transition state relatively late. The activation energies from the corresponding precursor complex are in the order of **1FT** (54.6 kJ/mol) < **1OT** (121.2 kJ/mol) < **1NT** (187.7 kJ/mol). Also, the energies of **1FT**, **1OT**, and **1NT** are above those of

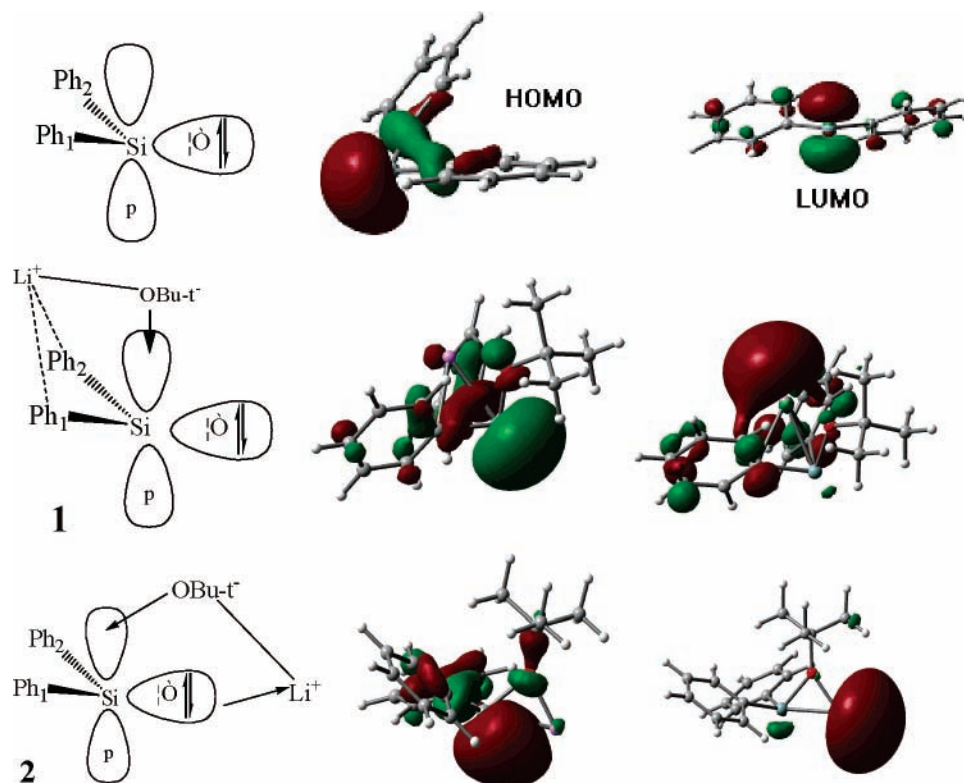
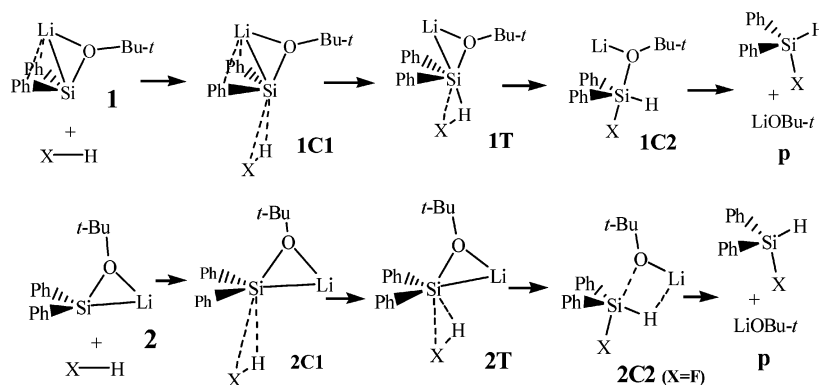


Figure 1. Frontier molecular orbital analyses of the singlet silylene Ph_2Si , the p -complex (**1**) and the three-membered ring (**2**) isomers of silylenoid $\text{Ph}_2\text{SiLi}(\text{OBu-}t)$, HOMO (middle) and LUMO (right).

SCHEME 1



the reactants (**1** + XH) by -1.3 , 87.4 , and 167.7 kJ/mol, respectively. On this basis, one can therefore conclude that the **1** insertion reaction into XH (X = F, OH) is essentially more favorable than that into NH_3 . Consequently, our theoretical results are in complete accord with the Hammond postulate,¹² which associates a reactant-like transition state with a smaller barrier and a more exothermic reaction (vide infra).

In comparison with those of the precursor complexes, the positive charge of the Si atom in transition states increases by

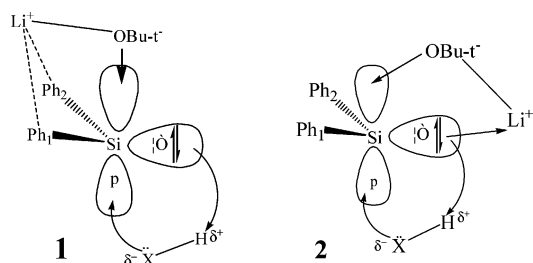


Figure 2. Schematic representations of the interactions between $\text{Ph}_2\text{-SiLi}(\text{OBu-}t)$ (**1** and **2**) and X–H bond.

0.358 (**1FT**), 0.392 (**1OT**), and 0.395 (**1NT**), whereas the electron charges of the H atom and the X group decrease by 0.391 and 0.065 in **1FT**, 0.398 and 0.115 in **1OT**, and 0.359 and 0.167 in **1NT**. That is, there exists an electron transfer of $\text{Si} \rightarrow \text{H} \rightarrow \text{X}$ in the transition state (see Figure 2). The occupancy numbers of the Si–H bond formed in **1FT**, **1OT**, and **1NT** are 1.923 , 1.919 , and 1.918 , respectively. However, the Si–X interaction is still very weak. It is indicated that the Si–H bond formed earlier than the Si–X bond.

3.1.3. Insertion Intermediates. After getting over the transition state, the Si–X bond forms gradually with the H–X bond rupturing. The $\text{LiOBu-}t$ moiety separates gradually away from the Si atom with the Li–O distance reducing. Then, the insertion intermediate is formed. Geometries of three intermediates, **1FC2**, **1OC2**, and **1NC2**, are similar (see Figures 3 and 4). Most of the σ electrons on the Si atom are transferred to an H atom, causing the Si atom have 1.781 (**1FC2**), 1.748 (**1OC2**), and 1.756 (**1NC2**) positive charges. The process from transition state to intermediate is also that of X reacting with Si from the back of the O atom. In the intermediate, the Si–X distances

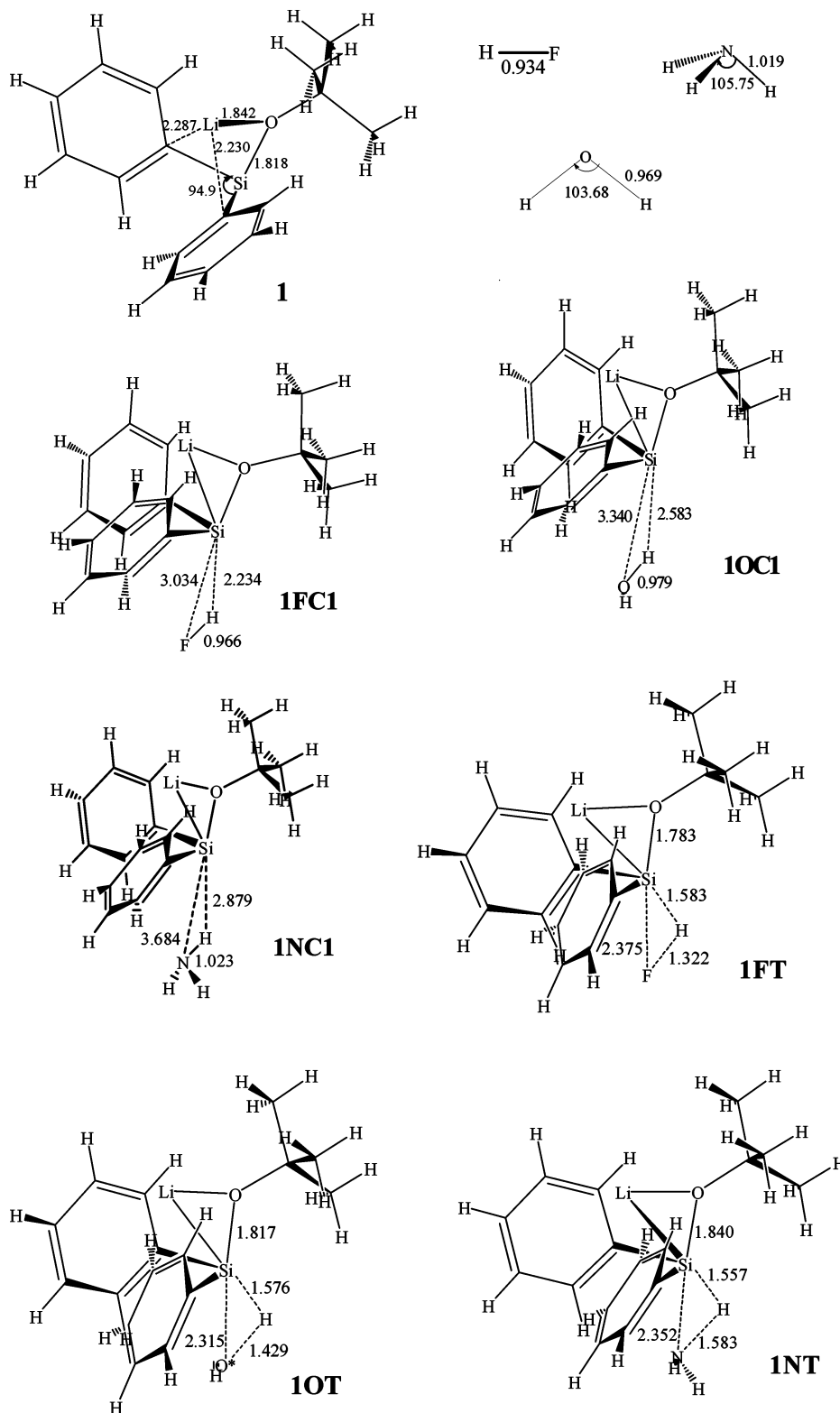


Figure 3. Optimized geometries (bond length, Å; bond angle, deg) of the reactions of **1** + XH ($X = F, OH, NH_2$) at the B3LYP/6-31G(d) level.

have greatly shortened to 1.692 Å (**1FC2**), 1.742 Å (**1OC2**), and 1.750 Å (**1NC2**), which are almost equal to that in corresponding product Ph_2SiHX (see Figures 3 and 4). In addition, the Si–O distance increases obviously, and the interaction between them has become weak. So, the process discussed above is similar to an S_N2 -type reaction mechanism. In fact, the intermediate can be regarded as an electrostatic complex of silane Ph_2SiHX with $LiOBU-t$. The relative energy

of intermediate increases in the order of **1FC2** (–239.2 kJ/mol) < **1OC2** (–135.2 kJ/mol) < **1NC2** (–60.3 kJ/mol).

3.1.4. Insertion Products. When the $LiOBU-t$ moiety separates away completely from the Si atom, the silane Ph_2SiHX can be obtained. The theoretical results show that all the insertion products Ph_2SiHX adopt a tetra-coordinate conformation on the silicon center (see Figures 3 and 4). As shown in Table 1, all the insertion reactions of **1** into XH ($X = F, OH, NH_2$) are

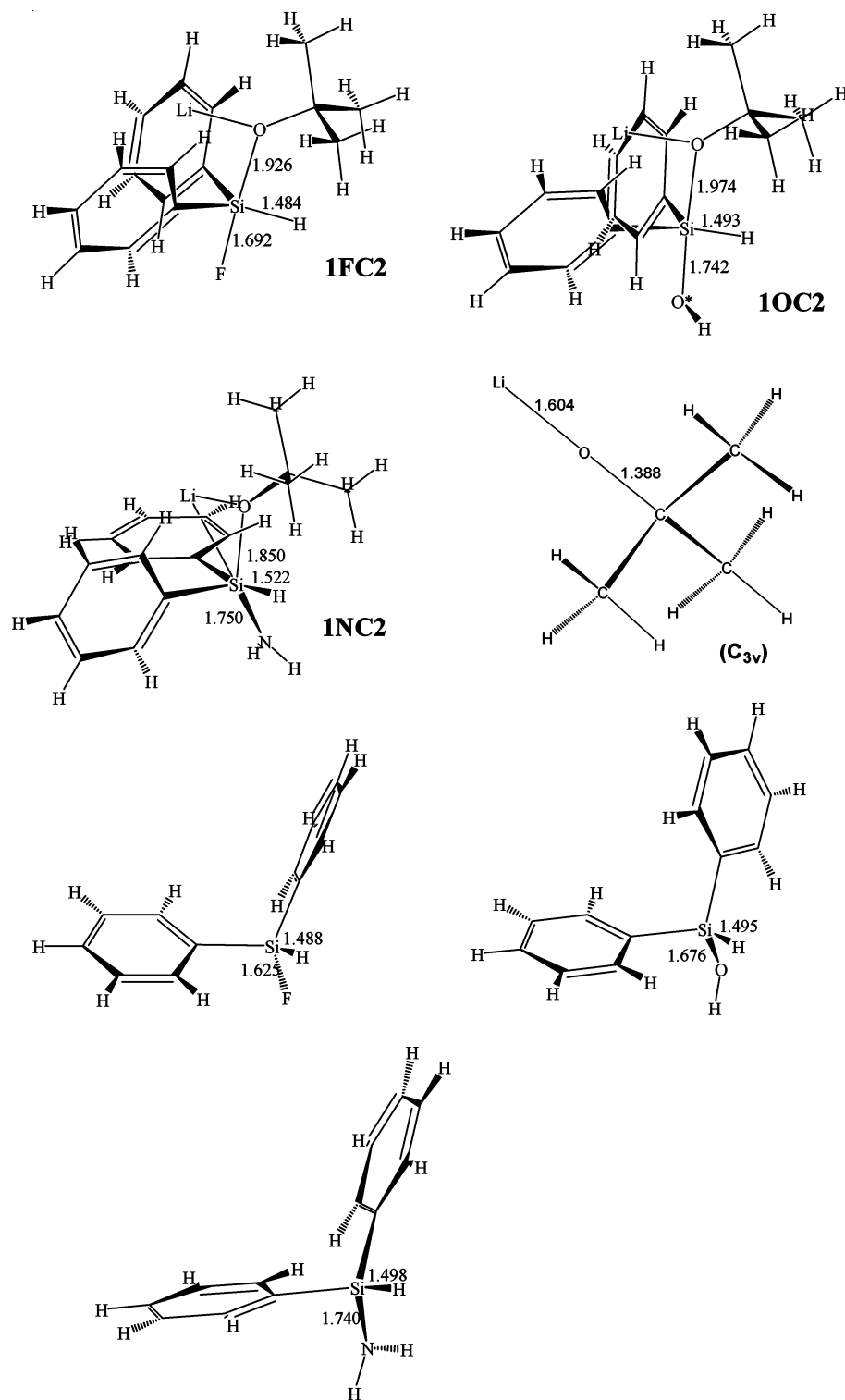


Figure 4. Optimized geometries (bond length, Å; bond angle, deg) of the reactions of **1** + XH (X = F, OH, NH₂) at the B3LYP/6-31G(d) level.

exothermic. The smallest enthalpy is the insertion reaction of **1** + NH₃ system (−47.0 kJ/mol). The highest exothermicity is predicted for the **1** + HF system (−180.8 kJ/mol). These results suggest even more that **1** insertion into HF proceed most easily in three insertion reactions.

3.2. Insertions of 2 into X–H bonds (X = F, OH, and NH₂). The three-membered-ring structure **2** is the most basal isomer, and all the other isomers can interconvert with each other through it.^{2d} **2** can be considered a complex of the singlet Ph₂Si with compound LiOBu-*t*, where the positive Li atom and the negative O atom of LiOBu-*t* act on the lone-pair σ orbital

and the unoccupied p orbital of the singlet Ph₂Si (see Figure 1), respectively. The electron transfer O → Si → Li exists in **2**, which makes it stable. But its energy is calculated to be 30.9 kJ/mol higher than that of **1** at the B3LYP/6-31g(d) level. In **2**, the main component of the HOMO concentrates on the Si atom (the σ orbital LP_{Si} with occupancy number of 1.806), while that of the LUMO concentrates on the Li atom with a little part of it on the Si atom (the p orbital LP_{Si}* with occupancy number of 0.261). It is reasonable to say that **2** also has amphiphilic property in reactions, just like **1**. The three-membered ring would be a reactive center, because each bond in it is “loose” and weak.

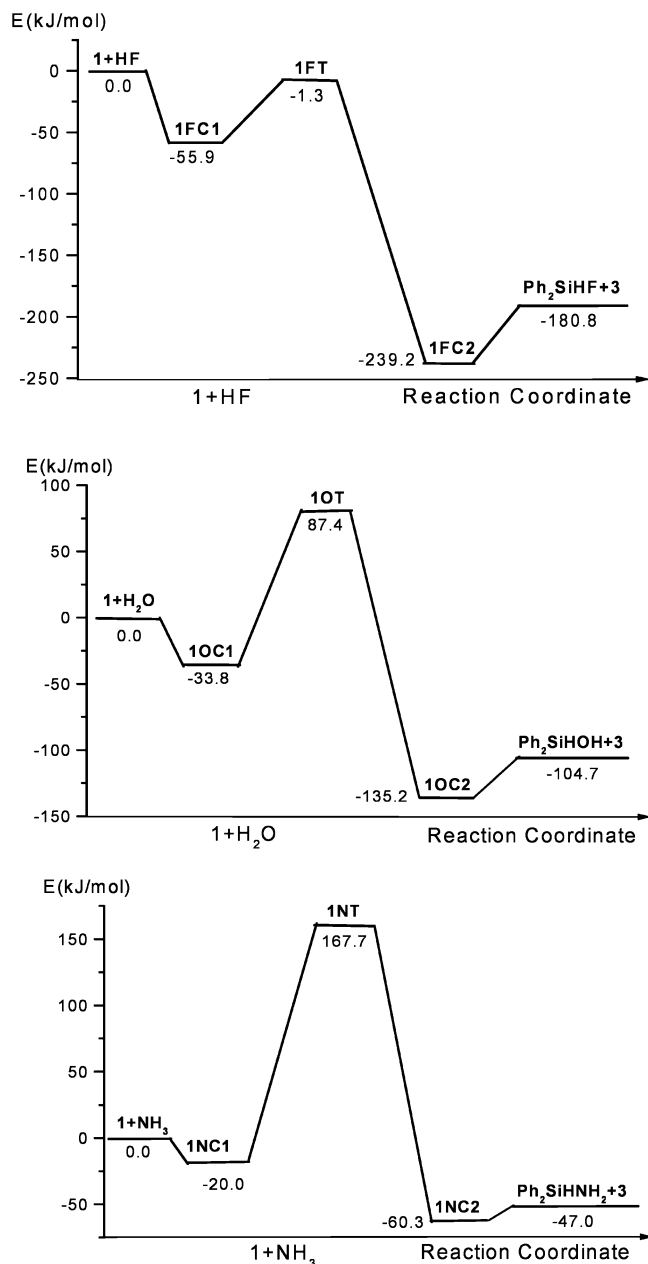


Figure 5. The schematic diagrams of the potential energy curves of the **1** + XH reactions (X = F, OH, NH₂) at the B3LYP/6-31G(d) level.

As shown in Scheme 1, the insertion reactions of **2** into X–H bonds take place under the Si atom.

3.2.1. Precursor Complexes. The initial formation of the precursor complex for the **2** + XH insertion is facilitated by the interaction between the low-lying p orbital (LUMO) on Si of **2** and the σ orbital (HOMO) of XH. As shown in Figure 6, in these precursor complexes, **2FC1**, **2OC1**, and **2NC1**, the Si–X distance decreases in the order of **2FC1** (3.445 Å) > **2OC1** (3.052 Å) > **2NC1** (2.711 Å), and the Si–H interaction is very weak. It can be found from Table 2 that the donation of σ electrons of XH into the p orbital on the Si atom does occur. In comparison with that of **2**, the positive charge of the Si atom decreases by 0.020 (**2OC1**) and 0.016 (**2NC1**), which corresponds to the occupancy number of LP*_{Si} increasing by 0.011 (**2OC1**) and 0.026 (**2NC1**). The stability energy (relative to the corresponding reactants) decreases in the order of **2FC1** (37.8 kJ/mol) > **2OC1** (29.4 kJ/mol) > **2NC1** (5.8 kJ/mol).

3.2.2. Transition States. As shown in Figure 2, two electron donation effects contribute to the proceeding of the

insertion reaction. One is the donation of the lone pair of electrons on X into the p orbital on the Si atom. The other is the donation of the σ electrons on the Si atom into the antibonding σ^* orbital (H atom of X–H bond). Then, transition states **2FT**, **2OT**, and **2NT** form (see Figure 6, oxygen in water is marked as O*), whose only imaginary frequencies are 1100i cm⁻¹(**2FT**), 1435i cm⁻¹(**2OT**), and 1577i cm⁻¹(**2NT**). In transition states, part of the σ electrons on the Si atom are transferred to the XH moiety, making the Si atom more positive, 1.303 (**2FT**), 1.333 (**2OT**), and 1.318 (**2NT**) (see Table 2). The Si–H bond distances are between 1.656 Å (**2OT**) and 1.679 Å (**2NT**). The occupancy numbers of the Si–H bond in **2FT**, **2OT**, and **2NT** are 1.875, 1.868, and 1.847, respectively. This suggests that the Si–H bond has nearly formed. On the other hand, the Si–X distance is in the order Si–F (2.278 Å) > Si–O* (2.165 Å) > Si–N (2.078 Å). Considering that the interaction between the Si atom and the center atom of the X group is the ligand effect, the Si–X distance mainly depends on the strength of the ligand. The strongest one is nitrogen in NH₃ and the weakest is fluorine in HF. Therefore, it does not come as a surprise that the Si–F bond distance in **2FT** is longer than the Si–O* distance in **2OT** and Si–N distance in **2NT**. The breaking X–H bond is stretched by 31.56% (**2FT**), 36.74% (**2OT**), and 36.90% (**2NT**) relative to its equilibrium value in XH. On the basis of the Hammond postulate,¹² **2FT** should have the smallest and **2NT** the highest activation barrier. This was fully confirmed by the computation of activation barriers for these insertion reactions. The activation energies from the corresponding precursor complex are in the order 28.7 kJ/mol (**2FT**) < 100.3 kJ/mol (**2OT**) < 143.3 kJ/mol (**2NT**). Also, the energies of **2FT**, **2OT**, and **2NT** are above those of the reactants (**2** + XH) by –9.1, 70.9, and 137.5 kJ/mol, respectively.

3.2.3. Insertion Intermediate and Products. After getting over the transition state **2FT**, Si–H and Si–F are formed gradually with the LiOBU-*t* moiety leaving from the Si atom and the H–F bond breaking off. The three-membered ring in **2** has been destroyed. The insertion intermediate **2FC** is formed (see Figure 6). In **2FC**, the O–Si distance is 2.021 Å, and the O–Li bond shortens near to that in compound LiOBU-*t*. Structure **2FC** can be considered a complex of silane Ph₂SiHF with compound LiOBU-*t*. The relative energy of **2FC** is –234.0 kJ/mol. With LiOBU-*t* being dissociated apart from **2FC**, the product silane Ph₂SiHF is obtained. The sum of the relative energies of Ph₂SiHF and LiOBU-*t* is –211.7 kJ/mol, and the reaction is highly exothermic. The intermediate structure, analogous to **2FC**, for the **2** + XH (X = OH, NH₂) system is not obtained. After passing through the transition state, the reaction leads to the separate products, Ph₂SiHX (X = OH, NH₂) and LiOBU-*t*. The reaction is exothermic by 135.6 kJ/mol for the **2** + H₂O system and 77.9 kJ/mol for the **2** + NH₃ system.

3.3. Comparison between 1 and 2 Insertions. Both **1** and **2** insertions into X–H bonds (X = F, OH, and NH₂) proceed in a concerted manner via a three-membered-ring transition state to form the same product, substituted silane Ph₂SiHX with dissociation of LiOBU-*t* (see Figure 2). There is a very clear trend toward lower activation barriers and higher exothermicity on going from NH₃ to H₂O to HF for **1** and **2** insertions. The explanation is connected with the nature of the XH hydrides and with steric effects. Electronegativity of the center atom of the X groups is in the order F > O > N. So, the H atom of the F–H bond has more positive charge. As shown in Figure 2, it is easier for the high-lying σ orbital and the low-lying p orbital on the Si atom to interact with the F–H bond than with O–H and N–H bonds. This interaction results in a lower barrier height

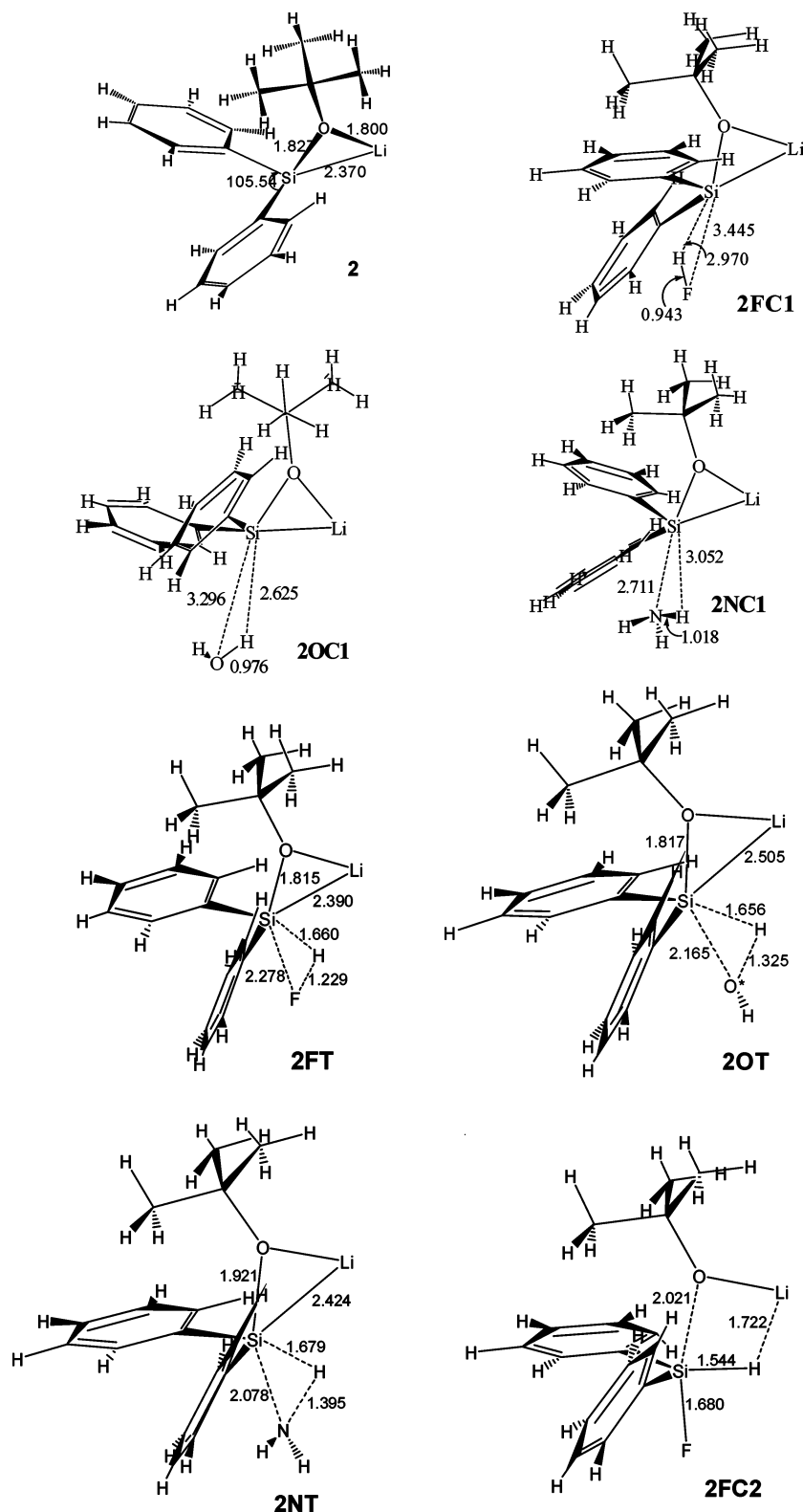


Figure 6. Optimized geometries (bond length, Å; bond angle, deg) of the reactions of **2** + XH (X = F, OH, NH₂) at the B3LYP/6-31G(d) level.

for HF insertion. On the other hand, it is relatively difficult for **1** or **2** to approach the NH₃ molecule, considering the steric factor, and a higher barrier is therefore expected.

As shown in Figure 2, both **1** and **2** isomers have amphiphilic property, nucleophilicity in the high-lying σ orbital direction and electrophilicity in the low-lying p orbital direction. The activation energies of **1** insertions are higher than those of **2** corresponding insertions by 7.8 kJ/mol (HF), 16.5 kJ/mol (H₂O),

and 30.7 kJ/mol (NH₃), respectively (see Figures 5 and 7). That is to say, structure **2** is more favorable for the insertion reactions of silylenoid Ph₂SiLi(OBu-*t*) into the X–H bonds (X = F, OH, and NH₂). According to the FMO theory,¹³ the reaction should be governed by the energy difference between the HOMO of one reactant and the LUMO of the other. Therefore, we examined the FMO energy difference between reactants at B3LYP/6-31g(d) level. As the results in Table 3 demonstrate,

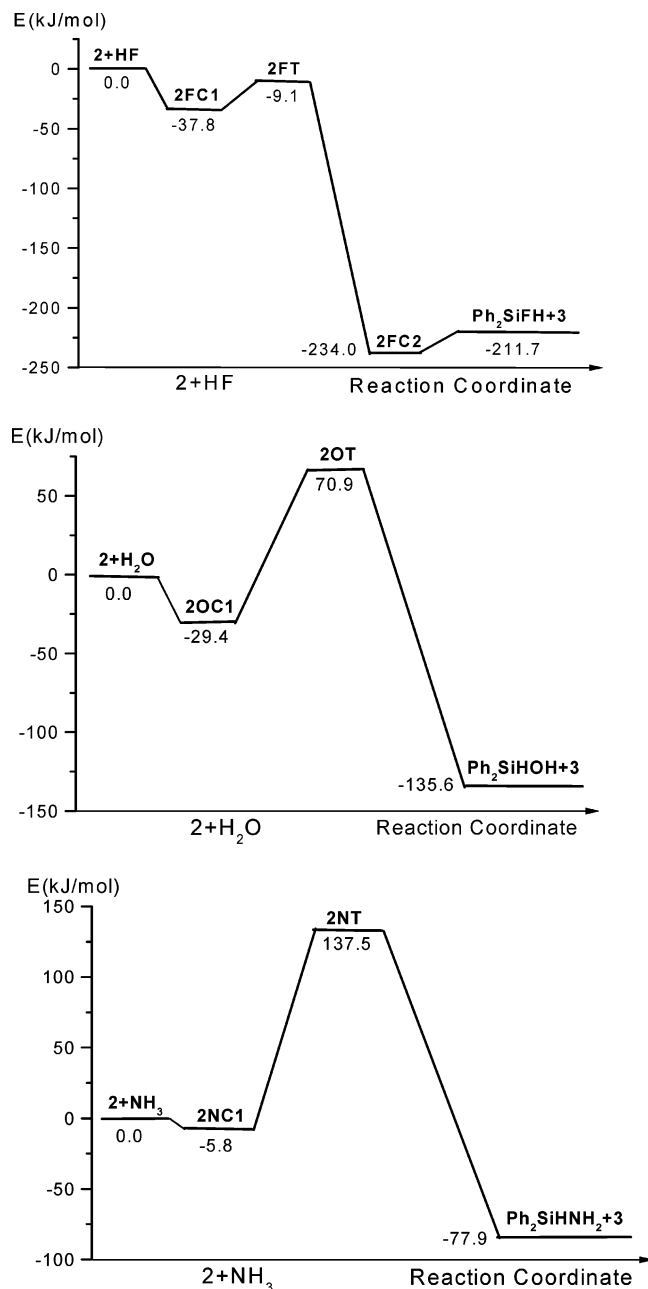


Figure 7. The schematic diagrams of the potential energy curves of the **2** + XH reactions (X = F, OH, NH₂) at the B3LYP/6-31G(d) level.

TABLE 3: Frontier Molecular Energies (au) for the Reactants and Their Differences between the Reactants Computed at B3LYP/6-31G(d) Method^a

reactants	HOMO _I	LUMO _I	HOMO _{XH}	LUMO _{XH}	ΔFMO_A	ΔFMO_B
1 + HF	-0.16660	-0.02279	-0.37623	0.06165	0.35344	0.22825
1 + H ₂ O	-0.16660	-0.02279	-0.29118	0.06262	0.26839	0.25922
1 + NH ₃	-0.16660	-0.02279	-0.25240	0.07860	0.22961	0.24520
2 + HF	-0.16467	-0.04221	-0.37623	0.06165	0.33402	0.22632
2 + H ₂ O	-0.16467	-0.04221	-0.29118	0.06262	0.24897	0.25729
2 + NH ₃	-0.16467	-0.04221	-0.25240	0.07860	0.21019	0.24327

^a ΔFMO_A = energy difference between LUMO_I of corresponding isomer (**1** or **2**) and HOMO_{XH} of reactant XH (HF, H₂O, or NH₃). ΔFMO_B = energy difference between LUMO_{XH} reactant XH and HOMO_I of corresponding isomer.

the lower FMO energy gap (ΔFMO_A or ΔFMO_B) was computed to be **2** as the reactant. Therefore, the **2** insertion barriers should be lower than those of the corresponding **1** insertions.

4. Concluding Remarks

1. Both **1** and **2** insertions into X–H bonds (X = F, OH, and NH₂) proceed in a concerted manner to form the substituted silane Ph₂SiHX with dissociation of LiOBu-*t*. All insertion reactions are exothermic.

2. The order of reactivity by **1** or **2** insertion is HF > H₂O > NH₃. The results can be easily understood in terms of electronic and steric effects.

3. Both **1** and **2** isomers have amphilic property, nucleophilicity in the high-lying σ orbital direction and electrophilicity in the low-lying p orbital direction. **2** is more reactive in the insertion reactions into X–H bonds (X = F, OH, and NH₂).

These findings in this paper prompt us to understand the reactivity of silylenoid. In this case, silylenoid Ph₂SiLi(OBu-*t*) reacts with HF easily, considering its barrier height. So, it could be detected just at very low temperature.³

Acknowledgment. This work was supported financially by the National Nature Science Foundation of China (no. 20373034), PhD Special Research Foundation of Chinese Education Department, and High Performance Computational Center of Shandong University.

References and Notes

- Clark, T.; Schleyer, P. R. *J. Organomet. Chem.* **1980**, *191*, 347.
- (a) Feng, S. Y.; Ju, G. Z.; Deng, C. H. *Chem. Phys. Lett.* **1991**, *186*, 248. (b) Feng, S. Y.; Feng, D. C.; Li, J. H. *Chem. Phys. Lett.* **2000**, *316*, 146. (c) Feng, S. Y.; Zhou, Y. F.; Feng, D. C. *J. Phys. Chem. A* **2003**, *107*, 4116. (d) Feng, D. C.; Xie, J.; Feng, S. Y. *Chem. Phys. Lett.* **2004**, *396*, 245.
- Tamao, K.; Kawachi, A. *Angew. Chem., Int. Ed. Engl.* **1995**, *34*, 818.
- Lee, M. E.; Cho, H. M.; Lim, Y. M.; Choi, J. K.; Park, C. H.; Jeong, S. E.; Lee, U. *Chem. Eur. J.* **2004**, *10*, 377.
- (a) Likhar, P. R.; Zirngast, M.; Baumgartner, J.; Marschner, C. *Chem. Commun.* **2004**, 1764. (b) Kawachi, A.; Oishi, Y.; Kataoka, T.; Tamao, K. *Organometallics* **2004**, *23*, 2949.
- Tanaka, Y.; Kawachi, A.; Hada, M.; Nakatsuji, H.; Tamao, K. *Organometallics*, **1998**, *17*, 4573.
- Tamao, K.; Kawachi, A.; Asahara, M.; Toshimitsu, A. *Pure Appl. Chem.* **1999**, *71*(3), 393.
- (a) Beck, A. D. *J. Chem. Phys.* **1993**, *98*, 5648. (b) Beck, A. D. *Phys. Rev. A* **1988**, *38*, 3098. (c) Vosko, S. H.; Wilk, L.; Nusair, M. *Can. J. Phys.* **1980**, *58*, 1200. (d) Lee, C.; Yang, W.; Parr, R. G. *Phys. Rev. B* **1988**, *37*, 785.
- (a) Gonzalez, C.; Schlegel, H. B. *J. Chem. Phys.* **1989**, *90*, 2154. (b) Gonzalez, C.; Schlegel, H. B. *J. Phys. Chem.* **1990**, *94*, 5523.
- (a) Weinhold, F. *Natural Bond Orbital Methods*. In *Encyclopedia of Computational Chemistry*; Schleyer, P. v. R., Ed.; Wiley: Chichester, 1998; Vol. 3, pp 1792–1811. (b) Glendening, E. D.; Badenhoop, J. K.; Reed, A. E.; Carpenter, J. E.; Weinhold, F. *NBO*, version 3.1, Theoretical Chemistry Institute, University of Wisconsin, Madison, 1995.
- Frisch, M. J.; Trucks, G. W.; Schlegel, H. B.; Scuseria, G. E.; Robb, M. A.; Cheeseman, J. R.; Montgomery, J. A., Jr.; Vreven, T.; Kudin, K. N.; Burant, J. C.; Millam, J. M.; Iyengar, S. S.; Tomasi, J.; Barone, V.; Mennucci, B.; Cossi, M.; Scalmani, G.; Rega, N.; Petersson, G. A.; Nakatsuji, H.; Hada, M.; Ehara, M.; Toyota, K.; Fukuda, R.; Hasegawa, J.; Ishida, M.; Nakajima, T.; Honda, Y.; Kitao, O.; Nakai, H.; Klene, M.; Li, X.; Knox, J. E.; Hratchian, H. P.; Cross, J. B.; Bakken, V.; Adamo, C.; Jaramillo, J.; Gomperts, R.; Stratmann, R. E.; Yazyev, O.; Austin, A. J.; Cammi, R.; Pomelli, C.; Ochterski, J. W.; Ayala, P. Y.; Morokuma, K.; Voth, G. A.; Salvador, P.; Dannenberg, J. J.; Zakrzewski, V. G.; Dapprich, S.; Daniels, A. D.; Strain, M. C.; Farkas, O.; Malick, D. K.; Rabuck, A. D.; Raghavachari, K.; Foresman, J. B.; Ortiz, J. V.; Cui, Q.; Baboul, A. G.; Clifford, S.; Cioslowski, J.; Stefanov, B. B.; Liu, G.; Liashenko, A.; Piskorz, P.; Komaromi, I.; Martin, R. L.; Fox, D. J.; Keith, T.; Al-Laham, M. A.; Peng, C. Y.; Nanayakkara, A.; Challacombe, M.; Gill, P. M. W.; Johnson, B.; Chen, W.; Wong, M. W.; Gonzalez, C.; Pople, J. A. *Gaussian 03*, revision C.02; Gaussian, Inc.: Wallingford, CT, 2004.
- Hammond, G. S. *J. Am. Chem. Soc.* **1955**, *77*, 334.
- Fukui, K.; Fujimoto, H. In *Mechanisms of Molecular Migration*; Thyagarajan, B. S., Ed.; Interscience: New York, 1968; Vol. 2. Fukui, K. *Acc. Chem. Res.* **1971**, *4*, 57. Fukui, K. *Angew. Chem., Int. Ed. Engl.* **1982**, *21*, 801.